

3.2.2 Large-Signal Design

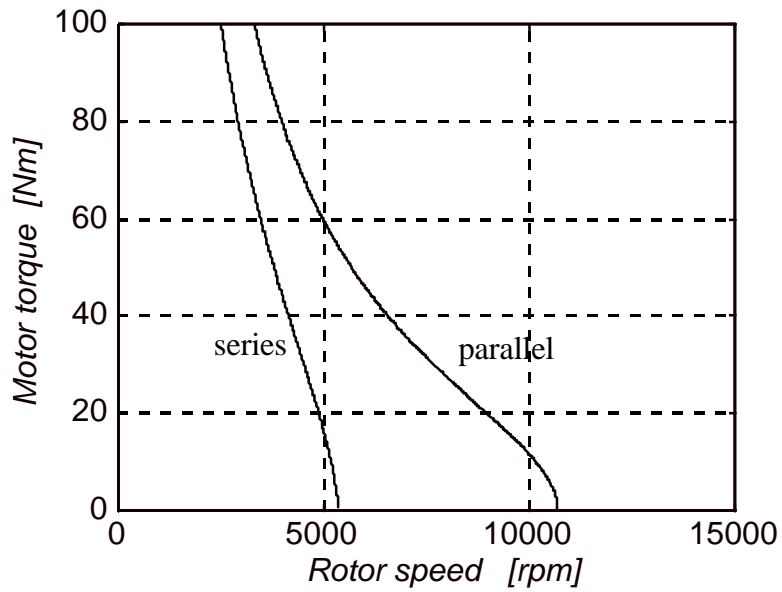
A large-signal design considers the time-domain behavior of the controlled PMSM drive under different working conditions [4, 5, 10, 18]. It also considers non-linear control parts which are supposed to be of small influence to the system small-signal response, but significantly determine its large-signal behavior. Those parts are a flux-weakening controller, integrator reset loops in the VLPI regulators and voltage and current limiters. Also, the system behavior is analyzed in two operating modes determined by series and parallel stator winding connections. Because the motor parameters are different, the small signal analysis and controller design must be completed for both cases. The benefits of switching from one to the other operating mode are discussed later in this section. An example of large-signal design and system time domain simulations is given in Chapter 4. For the sake of simplicity, only torque controlled (open speed loop) system is simulated.

3.2.2.1 Natural Output (Torque vs. Speed) Characteristics of The PMSM

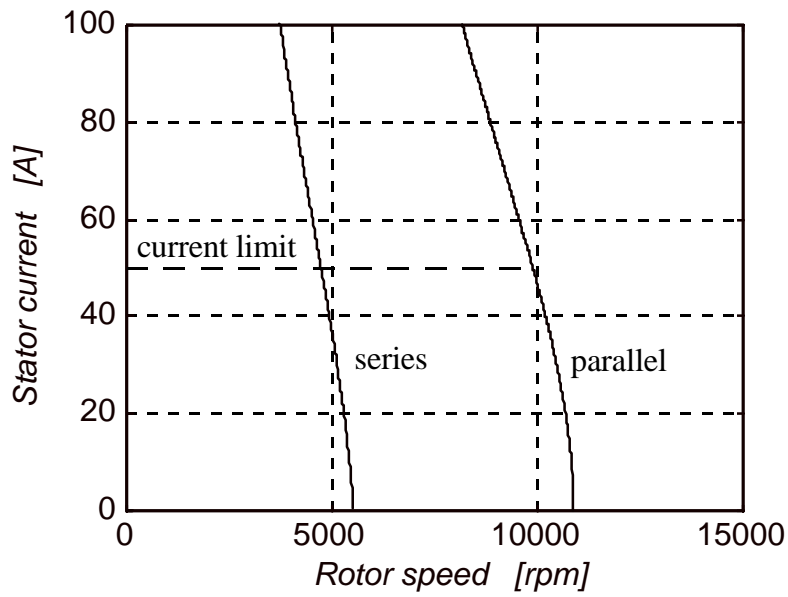
This examination of the output (Torque versus Speed) characteristics of the PMSM is necessary to get a feeling for a the motor operating limitations, i.e. its safe operating area (SOA), and, consequently, to determine base speed values (rated speed) for the beginnings of the flux-weakening in both operating modes. The motor is represented here by the steady-state part of its state-space voltage Eq.s (62). For the sake of simplicity, it is set that $i_d = 0$.

$$\begin{aligned}
 v_d &= -pL_q \omega i_q ; \quad v_q = Ri_q + k_t \omega \\
 T_m &= \frac{3}{2} k_t i_q ; \quad T_m - T_{load} - T_{fr} = 0 \\
 v_s &= \sqrt{v_d^2 + v_q^2} = V_{ph} ; \quad v_{smax} = mV_{dc} \\
 i_s &= \sqrt{i_d^2 + i_q^2} = I_{ph}
 \end{aligned} \tag{62}$$

The area within the boundaries determined by the motor maximum voltage and maximum current, Figure 23, is called the SOA of the motor [57]. Usually, in a converter-fed motor drive, the current limit of the converter is lower than the one of the motor, so it is used as a current boundary of the drive system [42, 65].



a) Motor torque characteristics



b) Stator current characteristics

Figure 23. Natural output characteristics of a PMSM for series and parallel winding connections and $i_d=0$

A motor speed at the moment when the voltage v_s reaches its limit (nominal value), v_{smax} , under maximum operating current (nominal value), i_{smax} , is called the rated (base) speed, ω_b , Figure 23. During the motor start-up (at zero speed), the transient current is allowed to be approximately twice its nominal value, but it will not be considered here for the sake of simplicity. It will be shown in Section 3.2.3 that the SOA can be extended for higher speeds using flux-weakening control methods. The base speed is used to be the starting point of a flux-weakening region. It should be noted from the motor output characteristics given in Figure 23, that the shape of SOA depends on the motor parameters as well as voltage and current limits. That consideration should be applied when choosing or designing the motor for the desired application.

3.2.2.2 PMSM Current and Voltage Vector Diagrams in DQ Coordinates

Current and voltage polar plots in d-q coordinate space are useful characteristics for the PMSM drive design in order to understand the interactions between the motor nature and current and voltage limitations [41, 47-49, 58]. They are applied especially for flux-weakening control design [63-71], discussed in Section 3.2.3.

An interior permanent magnet (IPM) motor current and voltage limits can be explained through their polar diagrams, given in Figure 24 and Figure 25, respectively. The circles on the diagrams represent current and voltage limits due to their maximum vector magnitudes. The families of ellipses are derived from the motor voltage d-q state-space Eq.s (12), with neglected stator resistance and current dynamics in the vicinity of operating points ($\frac{di_q}{dt}, \frac{di_d}{dt} \approx 0$), which is a generally applied approximation in flux-weakening designs [51, 65, 66, 69]. Each ellipse represents current and voltage limits due to the motor voltage state-space d-q model, Eq.s (12), at some interesting operating point (base (rated) speed, ω_b , critical speed, ω_{cr} , and maximum speed ω_{max}), which will be more closely defined in Section 3.2.3. Hence, the ellipses represent PMSM d-q current and voltage state-space limits in steady-state [51, 58, 65, 66]. The derivation of their analytical forms from Eq.s (12) is given in Eq.s (63) and (64) for current and voltage characteristics, respectively.

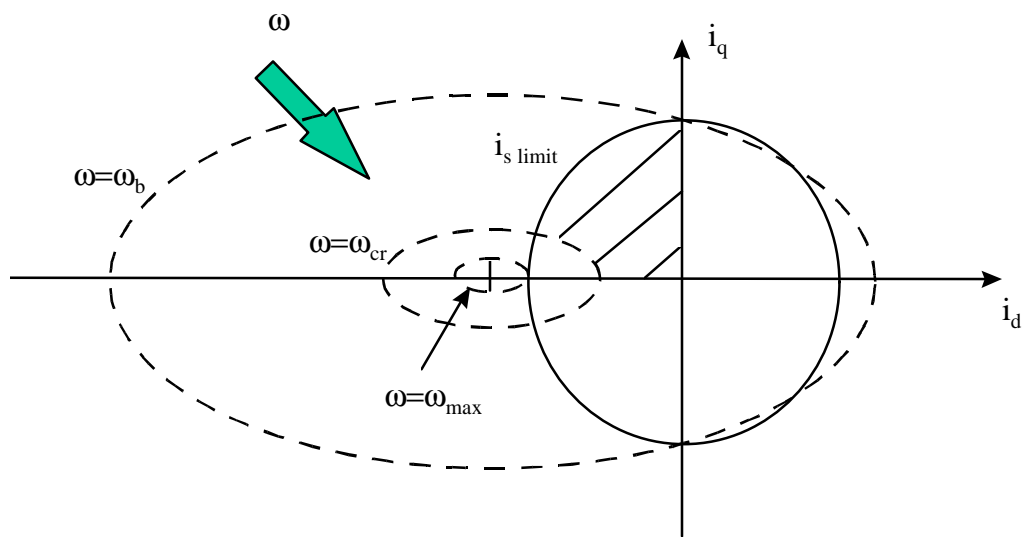


Figure 24. PMSM current limit d-q polar diagram

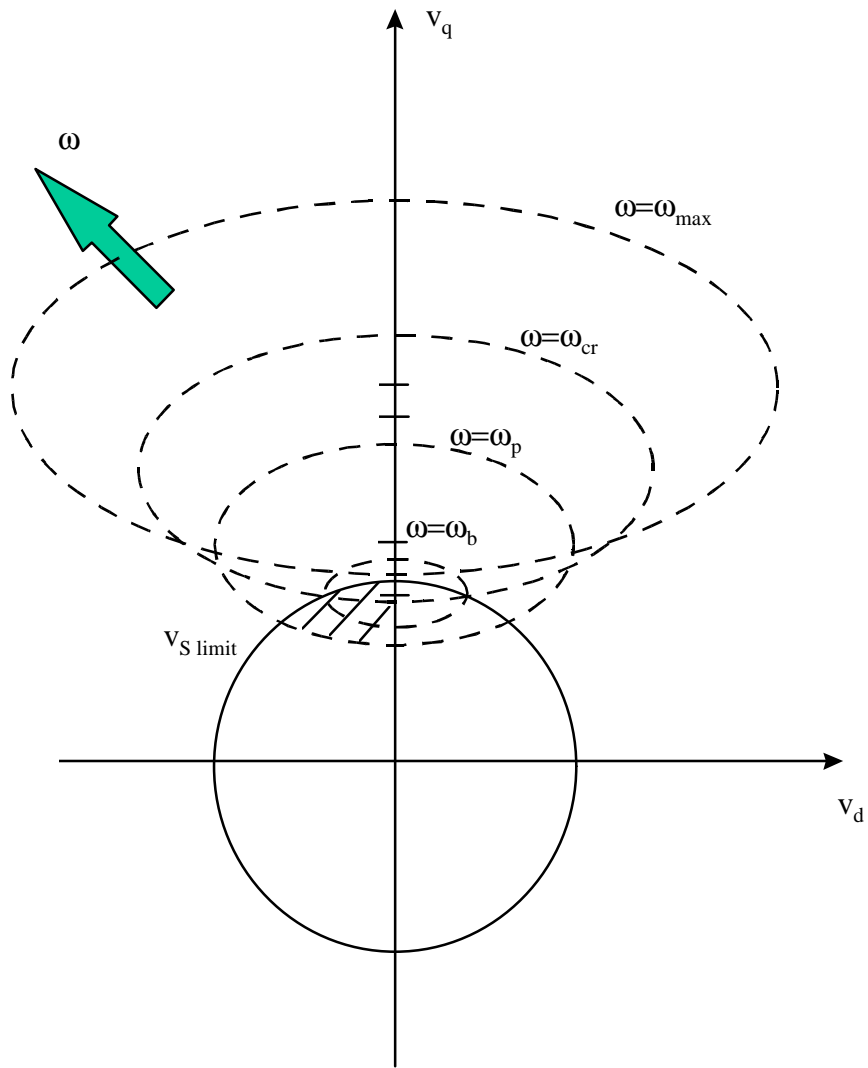


Figure 25. PMSM voltage limit d - q polar diagram

$$\begin{aligned}
\frac{v_d^2}{\mathbf{w}^2} &= (pL_q)^2 i_q^2 ; & \frac{v_q^2}{\mathbf{w}^2} &= (pL_d i_d + k_t)^2 \\
\frac{V_s^2}{\mathbf{w}^2} &= (pL_q)^2 i_q^2 + (pL_d)^2 (i_d + \frac{k_t}{pL_d})^2 \\
a &= \frac{V_s}{pL_q \mathbf{w}} ; & b &= \frac{V_s}{pL_d \mathbf{w}} ; & c &= \frac{k_t}{pL_d} \\
\boxed{\frac{i_q^2}{a^2} + \frac{(i_d + c)^2}{b^2} = I} & & & & (63)
\end{aligned}$$

$$\begin{aligned}
i_d &= \frac{v_q - k_t \mathbf{w}}{pL_d \mathbf{w}} ; & i_q &= -\frac{v_d}{pL_q \mathbf{w}} \\
I_s^2 &= \frac{(v_q - k_t \mathbf{w})^2}{(pL_d \mathbf{w})^2} + \frac{v_d^2}{(pL_q \mathbf{w})^2} \\
a &= \frac{pL_d \mathbf{w}}{I_s} ; & b &= \frac{pL_q \mathbf{w}}{I_s} ; & c &= k_t \mathbf{w} \\
\boxed{\frac{(v_q - c)^2}{a^2} + \frac{v_d^2}{b^2} = I} & & & & (64)
\end{aligned}$$

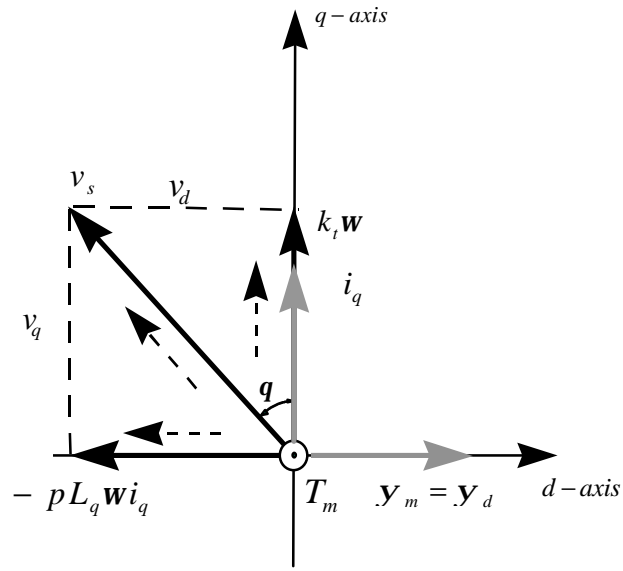
It should be noticed from Eq. (63) that the current ellipse axes, a and b, decrease with speed and that the center location is on the negative d-semiaxis and it is constant, i.e. the current state-space limits are concentric ellipses, with speed as a parameter. On the other hand, it can be seen from Eq. (64) that the voltage ellipse axes, a and b, increase with speed, as well as that their centers, which are equal to the motor back emf at a given speed, located on the positive q-semiaxis, move further from the origin. These phenomena are easy to explain from voltage d-q state-space equations, (12). In order to increase speed while keeping voltage constant, the current must decrease and, inversely, if the current should be constant, the voltage must increase with speed. This explains the current and voltage ellipse axes relationships with speed in Eq.s (63) and (64). However, the behavior of the ellipse centers releases an interesting phenomenon. The only reason for the ellipse eccentricity in the d-q plane, in both cases, is the existence of motor back emf, $k_t \mathbf{w}$, Eq.s (12). At zero speed the back emf is also zero and the center of the hypothetical voltage ellipse, which has collapsed to a single point, is at the origin, what is expected. However, the center of the current ellipse depends only on motor parameters - back emf constant, k_t ,

number of pole pairs, p , and d-axis inductance, L_d - but not speed, so that whatever back emf is developed, the center stays the same for the same motor. Moreover, since the current ellipses collapse with increasing speed, it converges to that point [58, 69]. The following discussion will show that it helps a lot in flux-weakening control design. On the other hand, the voltage limit diagram, Figure 25, helps in the design of a constant current flux-weakening control strategy [66]. It should be noted that there are two distinguished speed regions: one where the relative speed increase is higher than the relative i_q current (motor torque) decrease, which includes an increasing or constant current (motor torque) region, causing a v_d voltage increase, and the other, where the torque decreases faster than the speed increases, so that the v_d voltage decreases, so that the phase voltage vector moves toward a positive q-semiaxis. The passing point between the two regions, speed ω_p , can be calculated from Eq.s (12), which will be explained in Section 3.2.3. A PMSM voltage d-q vector diagram, developed from Eq.s (12), is shown in Figure 26 - for the maximum torque operating region (for the sake of simplicity, it was approximated with $i_d=0$ condition), Figure 26.a, and the flux-weakening region, Figure 26.b. The current and voltage vectors cannot exceed the limits from Figures 24 and 25. The voltage diagrams, as well as the SOA diagrams completely describe the PMSM drive. They are the basis for understanding the PMSM drive system behavior, which is the prerequisite for the large-signal design.

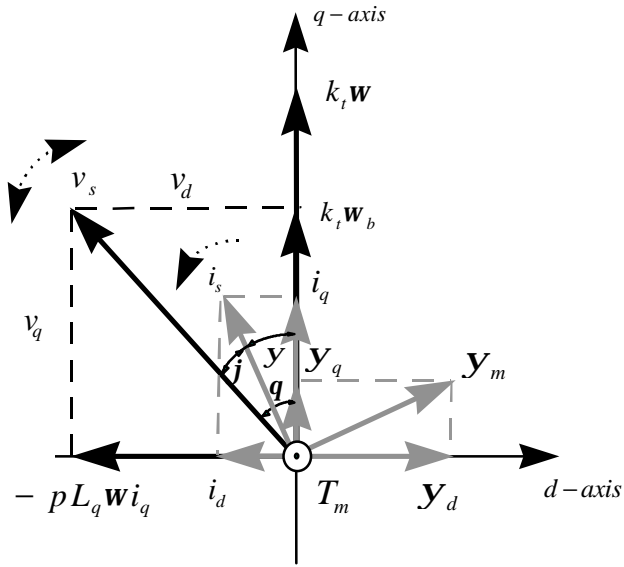
3. Reference Motor Torque Profile

In order to minimize energy consumption, the motor torque should keep its maximum value until the rated speed is reached, except during the relatively short time periods when it rises from zero to the maximum value with a certain maximum slope, determined by mechanical limitations of the motor drive system [4, 42, 64, 70, 71]. The validation for that suggestion lies in the minimum energy (noted as E) Eq. (65), which is derived from Eq.s (12):

$$\begin{aligned} \min E &= \min \int_{t_1}^{t_2} P_m dt = \frac{1}{J} \min \int_{w_1}^{w_2} \frac{w}{T_{load} + T_{fr} - T_m} dw \\ w_1 &= \frac{1}{J} (T_{mb} - T_{loadb} - T_{frb}) t_1 = w_b, \quad x_b - \text{base value of } x \\ w_2 &= \frac{1}{J} (T_{m \text{ final}} - T_{load \text{ final}} - T_{fr \text{ final}}) t_2 = w_{\text{final}} (= w_{\text{max}}), \quad x_{\text{final}} - \text{final value of } x \end{aligned} \quad (65)$$



a) $i_d = 0$



b) $i_d \neq 0$

Figure 26. PMSM voltage d-q vector diagram for a) $i_d=0$ and b) $i_d \neq 0$

where P_m is the motor power, J motor inertia, ω motor speed, ω_1 and ω_2 motor speed values at time moments t_1 and t_2 , T_m , T_{load} and T_{fr} motor, load and friction torque, respectively, and x a common variable for ω , T_m , T_{load} and T_{fr} . The base and final values are related to base and final motor speed. It can be noticed from Eq. (65) that when $T_{load} \geq 0$, the energy consumption is lowest with the maximum motor torque. If $T_{load} < 0$, a trade-off must be made between minimum energy consumption and starting time period. If the reluctance torque component in Eq.s (12) is negligible, the maximum torque at a base speed usually means a maximum i_q current. It allows the largest flux-weakening region, Figure 26.b, which will be explained in Section 3.2.3. Hence, under a lower i_q current, the voltage-to-current phase shift is smaller in the out of flux-weakening region and it decreases more rapidly within the flux-weakening region than in the maximum i_q current case. So, it reaches its limit, determined by the VSI limitations [31, 65], under a lower speed than in the maximum i_q current case, if the flux-weakening begins at the same speed.

All the abovementioned facts provide a good reason to continue with maximum torque (or maximum i_q current) reference out of the flux-weakening region, as long as the speed profile is not important. Short time periods for the torque ramping from zero to its maximum value with a certain maximum slope, are necessary restrictions due to mechanical limitations on the motor shaft. As a protection, a ramp limiter and a maximum current limiter can be used.

3.2.2.4 VLPI Compensator

Variable limit proportional-integrated compensator (VLPI) is a PI compensator with a high gain in the feedback branch of the integrator reset loop [79, 80]. The loop is closed whenever the output of the compensator reaches its limit, shown in Figure 27. Then the integrator output is reset to an almost zero value. Otherwise, the reset loop remains open and the integrator keeps its original function and VLPI works as a classical PI compensator.

Its main distinction from a classical PI compensator with anti-windup is that the origin of the reset feedback branch is placed after the summator instead at the integrator output. The advantage of this replacement can be illustrated through the compensator transfer functions while working in a saturation mode. The values L_1 and L_2 from the VLPI block diagram from Figure 27

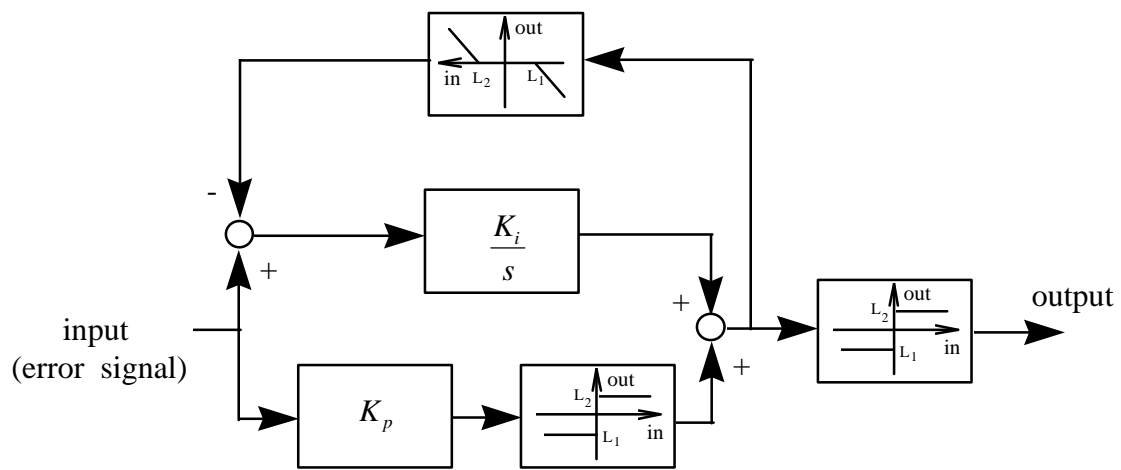


Figure 27. Block diagram of a variable limit PI regulator (VLPI)

represent the lower and upper compensator output limits. For the sake of simplicity, let's assume that $L_1 = L_2 = L_{max}$. Then, the proportional branch can be approximated as a constant L_{max} . Also, let's suppose that the output is not limited. Now, the transfer functions of the PI compensator with anti-windup and the VLPI compensator looks like Eq.s (66) and (67), respectively:

$$v_{out}(s) = \frac{1}{K_r} \frac{1}{\frac{s}{K_i K_r} + 1} v_{in}(s) + l(s) \quad (66)$$

$$v_{out}(s) = \frac{1}{K_r} \frac{1}{\frac{s}{K_i K_r} + 1} v_{in}(s) + \frac{1}{K_i K_r} \frac{s}{\frac{s}{K_i K_r} + 1} l(s) \quad (67)$$

where $v_{out}(s)$, $v_{in}(s)$ and $l(s)$ are the VLPI output, input and proportional branch signals, respectively, consisting of their large-signal (steady-state) and small-signal (perturbation) parts.

Unlike the output of the PI compensator with anti-windup, Eq. (66), which still needs to be limited to the L_{max} value, which introduces an additional non-linearity to the system main control-signal path, the VLPI compensator output, Eq. (67), is reduced to a very low value whenever it reaches its limit, which breaks the reset loop and tends to turn compensator back to the regular PI operating mode. Since the input signal is still high, it brings the compensator back to saturation, so that it oscillates around its limit value. The nature of the oscillations (frequency and amplitude) is determined by the reset and integral gains. Hence, the whole compensator is reset instead of only its integrator. It protects the compensator from hard saturation, and gives a faster compensator response to the input signal transients of entering and leaving the limit boundaries. A drawback of the VLPI is that a bad choice of the reset gain could produce the oscillations which introduce the uncertainty of the compensator operating point at the moment when it leaves the saturation mode.

3.2.2.5 Voltage Limitation

Voltage limitation is designed by defining and placing the VSI switching duty-cycle limiters in both the i_d and i_q current loops, which has maximum values of $|d_{dmax}| = |d_{qmax}| = 1$. From the discussion in Chapter 2 about modeling of the VSI and PWM modulator, it comes out that these limits should be scaled by the modulation coefficient, m , in order to obey the phase voltage limits and to avoid low harmonic distortions in the motor current and voltage signals (see

Appendix A) [11, 73, 78]. An additional limitation of the phase voltage vector magnitude, V_s , is necessary, because the vector addition of its two d-q component maximum magnitudes, V_d and V_q results in:

$$\sqrt{V_d^2 + V_q^2} = V_s \sqrt{2} \quad (68)$$

It can be solved in several ways. As an introduction to more complex optimization studies, which are left for future work, here is a brief overview of four of the most obvious duty-cycle limitation methods in d-q coordinates:

1) further control of the voltage v_q through its duty-cycle equivalent:

$$d_q = \sqrt{d_s^2 - d_d^2} \quad (69)$$

2) further control of the voltage v_d through its duty-cycle equivalent:

$$d_d = \sqrt{d_s^2 - d_q^2} \quad (70)$$

3) further control of the voltage v_s through its duty-cycle equivalent:

$$d_s = k \sqrt{d_q^2 + d_d^2} \leq 1 \quad (71)$$

through the linear decrease of its d-q components, where k is the linear limitation factor;

4) hard limitation of duty-cycle d-q components to the value $d_{max} = 1 / \sqrt{2}$.

Each method has different characteristics in constant-torque and flux-weakening regions, as is shown in Table 2. The arrows show increase or decrease of corresponding variable values. There are two observed cases at the flux-weakening region related to the v_q equation from Eq.s (12):

$$\begin{aligned} \text{a) } & \left| \frac{D\mathbf{w}}{\mathbf{w}} \right| < \left| \frac{D(k_t + pL_d i_d)}{k_t + pL_d i_d} \right|, \quad \text{and} \\ \text{b) } & \left| \frac{D\mathbf{w}}{\mathbf{w}} \right| > \left| \frac{D(k_t + pL_d i_d)}{k_t + pL_d i_d} \right|. \end{aligned}$$

As can be seen from Table 2, the influence of the limiting method to the motor drive behavior interacts with the chosen flux-weakening strategy and the load conditions. Consequently, there is no general rule for any voltage limitation method such as the one suggested in [63].

Table 2. Duty-cycle limitation methods

Limitation Method	CONSTANT TORQUE $i_q = \text{const.}; i_d = 0$	FLUX-WEAKENING $i_q \downarrow; -i_d \uparrow$	
		$\left \frac{Dw}{w} \right > \left \frac{Di_q}{i_q} \right $	$\left \frac{Dw}{w} \right < \left \frac{Di_q}{i_q} \right $
D _q Control	$w \uparrow; -d_d \uparrow \Rightarrow d_q \downarrow; w \downarrow$	a) $w \uparrow; -d_d \uparrow \Rightarrow d_q \downarrow; w \uparrow$ b) $w \uparrow; -d_d \uparrow \Rightarrow d_q \downarrow; w \downarrow$	a) $w \uparrow; -d_d \downarrow \Rightarrow d_q \downarrow; w \uparrow$ b) $w \uparrow; -d_d \downarrow \Rightarrow d_q \uparrow; w \uparrow$
D _d Control	$w \uparrow; d_q \uparrow \Rightarrow -d_d \downarrow; w \downarrow$	a) $w \uparrow; d_q \downarrow \Rightarrow -d_d \uparrow; w \uparrow$ b) $w \uparrow; d_q \uparrow \Rightarrow -d_d \downarrow; w \downarrow$	a) $w \uparrow; d_q \downarrow \Rightarrow -d_d \downarrow; w \uparrow$ b) $w \uparrow; d_q \uparrow \Rightarrow -d_d \downarrow; w \uparrow$
Linear Control	$w \uparrow; d_s \uparrow \Rightarrow a \downarrow; d_s \downarrow; w \downarrow$	a) $w \uparrow; d_s \downarrow \Rightarrow a \uparrow; d_s \downarrow; w \uparrow$ b) $w \uparrow; d_s \uparrow \Rightarrow a \downarrow; d_s \downarrow; w \downarrow$	a) $w \uparrow; d_s \downarrow \Rightarrow a \uparrow; d_s \uparrow; w \uparrow$ b) $w \uparrow; d_s \downarrow \Rightarrow a \uparrow; d_s \downarrow; w \uparrow$
Hard Limit	$w = w_{\text{rated}}; d_s = 1$	a) $w = w_{\text{max}}; d_s = 1$ b) $w = w_{\text{max}}; d_s = 1$	a) $w \uparrow; d_s = 1 \Rightarrow d_s \downarrow; w \uparrow$ b) $w = w_{\text{max}}; d_s = 1$

3.2.2.6 Series and Parallel Operating Modes

When the load torque profile allows a significant decrease of the motor torque at higher speed, as is the case with the load from Figure 14, the possibility of switching from series to parallel connection of the PMSM stator windings enables the reduction in the ratings of the VSI. In other words, it makes it possible to achieve higher maximum torque at lower speed (series connection) and higher maximum speed with lower torque (parallel connection) with the same maximum current and power. The maximum phase current of the motor can be limited to its maximum value for series winding connection, further called "series operating mode." The mathematical relations between series and parallel operating modes are:

$$\left. \begin{aligned}
T_m &= \frac{3}{2} k_t i_q \\
E_p &= k_{tp} \omega, E_s = 2 k_{ts} \omega \\
L \frac{di_L}{dt} &= k_t \omega \\
\text{series op. mode, } i_L &= i_q: \\
E_s &= \sum_j L_j \frac{di_q}{dt} \quad j = 1, 2 \\
\text{parallel op. mode, } i_L &= i_{qj}: \\
E_p &= L_j \frac{di_{qj}}{dt} \quad j = 1, 2 \\
i_q &= \sum_j i_{qj} \quad j = 1, 2 \\
L_j &= L = \text{const}
\end{aligned} \right\} \Rightarrow \left\{ \begin{aligned}
L_s &= 4L_p = 2L \\
E_s &= 4E_p = 4L_p \frac{di_q}{dt} \\
k_{ts} &= 2k_{tp}
\end{aligned} \right\} \Rightarrow i_{qs} = \frac{1}{2} i_{qp} \Big|_{T_m = \text{const}} \text{ or } T_{ms} = 2T_{mp} / i_m = \text{const}$$

(72)

p – parallel op. mode, s -series op. mode

where k_t , L , i_q , T_m , and ω are motor parameters and variables per single winding, listed in Table 1, subscripts s and p are for windings in series and parallel modes, respectively, and E is motor back emf. The idea is that there is a four times larger inductance in a series than in a parallel stator winding connection (in the case of two windings per phase), and four times higher back emf, consequently. That limits the motor rated speed to a two times lower value. On the other side, there is a two times higher motor torque in series than in parallel mode, which is important to start the motor from zero speed. If the load torque profile, such as the one from Figure 14, allows the motor torque reduction at high speed to more than two times a lower value, there is a possibility for motor drive optimization, so the switching from series to parallel operating mode can help to achieve a high speed and high torque profile (at low speed) with same, lower rated motor drive. This statement can be proved from Eq.s (63) and (72), and Figure 24. It can be seen that the same point in Figure 24 can be reached in series and parallel operating modes at proportionally different speed points, and under the same maximum (voltage and current) operating conditions.